AIAA 81-0383R

A Cost-Effective Method for Shock-Free Supercritical Wing Design

Pradeep Raj* and Luis R. Miranda†
Lockheed-California Company, Burbank, Calif.
and
A. Richard Seebass‡
University of Arizona, Tucson, Ariz.

A computationally efficient procedure for the design of shock-free supercritical wings is described. The method utilizes the fictitious-gas concept coupled with an improved version of the Jameson-Caughey full-potential finite-difference code, FLO-22, for analyzing three-dimensional wings. The computation of the velocity components at the plane of symmetry in the analysis code is modified to simulate the flow on isolated wings more accurately. In addition, the improved version of FLO-22 is capable of handling the wing-fuselage interference effect. The present design method computes the surface geometry beneath the supersonic region so as to eliminate the shock waves normally associated with transonic flight. Results for redesigned rectangular and swept wings are presented that indicate significant wave-drag reduction and improved aerodynamic characteristics when compared with the baseline wing.

Nomenclature

a	= real gas local speed of sound
a_f	= fictitious gas local speed of sound
a_*	= critical speed of sound
a_0	= stagnation speed of sound
b	= wing span
A,B,C,D,E,F	= coefficients in Eq. (4)
A_0,B_0,C_0,D_0	= coefficients in Eq. (14)
c	= chord
C_p	= coefficient of pressure
D	= drag
G	= reduced potential
k	= ratio of specific heats for ideal gas = 1.4
L	= parameter in fictitious gas sound speed law, Eq. (5); also lift
M_L	= local Mach number
M_∞	= freestream Mach number
R	= coefficient in Eq. (4)
(u,v,w)	= Cartesian components of local velocity vector
(x,y,z)	= Cartesian coordinates, x: chordwise, z: spanwise
Y_b	= new wing surface ordinate in computational plane
Y_s	= sonic surface height in computational plane
(X,Y,Z)	= mapped parabolic coordinate system
$(\bar{X},\bar{Y},\bar{Z})$	= transformed computational plane for supersonic flow calculation
$\alpha,\beta,\gamma,\delta$	= matrices, see Eq. (9)
θ	= angle of attack
μ	= parameter in Eq. (5)
Φ	= total velocity potential
∇	= gradient operator

Presented as Paper 81-0383 at the AIAA 19th Aerospace Sciences Meeting, St. Louis, Mo., Jan. 12-15, 1981; submitted March 4, 1981; revision received Aug. 17, 1981.

*Senior Aerodynamics Engineer. Member AIAA.
†Department Manager, Computational Aerodynamics. Member AIAA.
‡Professor, Aerospace Engineering and Mathematics. Associate Fellow AIAA.

Introduction

THE design of more energy-efficient transport aircraft has gained added importance in recent years due to a rapid increase of fuel cost. One of the major requirements for current aircraft designs is to increase the specific air range, that is, the distance flown per unit weight of fuel consumed. From an aerodynamic viewpoint, this can be accomplished by maximizing the range factor M_∞ (L/D). For subsonic cruise aircraft, the maximum value is achieved in transonic flight regime just before the onset of the transonic drag rise. However, once supersonic flow regions embedded in subsonic flow occur, shock waves are likely with the attendant wave drag and boundary-layer separation losses. The cruise efficiency of an aircraft will improve considerably if these shock waves are eliminated or made acceptably weak, as shown in Fig. 1. The improvement in aerodynamic efficiency may be

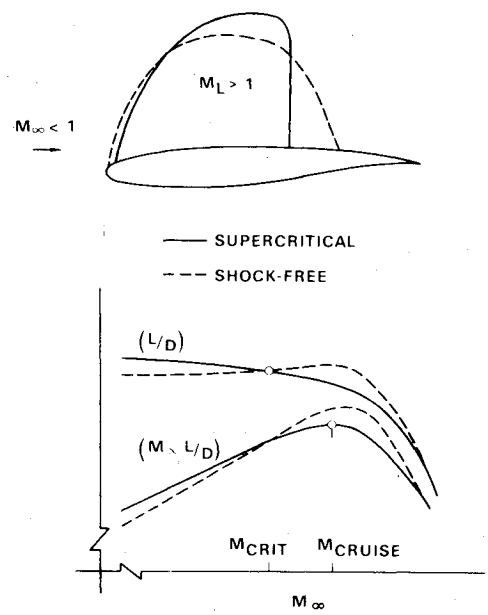

Fig. 1 Importance of shock-free transonic cruise.

traded for reduced structural weight by increasing the thickness of the shock-free supercritical wing or by decreasing the wing sweep compared with a conventional wing.

The development of practical "shock-free" airfoil sections was pioneered by the experimental research of Whitcomb[1] at the NASA Langley Research Center and Pearcy[2] at the National Physical Laboratory, United Kingdom. Subsequent analytical studies[3-6] based on hodograph method and computational studies,[7-12] using optimization technique and finite-difference methods, provide the design procedures for two-dimensional airfoils in inviscid transonic flow. As a consequence, the supercritical airfoil technology may be considered essentially fully developed. The implementation of these advances in aircraft wing design requires that the three-dimensionality of the flow be accurately incorporated. Progress in this area has been relatively limited owing to the lack of a hodograph-type technique and the high cost of computational explorations.

A direct design method based on repetitive application of a three-dimensional analysis code to various wing geometries is obviously very uneconomical. Hicks and Henne[13] and Lores et al.[14] present a more desirable design method that uses optimization technique in conjunction with an analysis code. The procedure seeks to minimize some specified parameters (e.g., the drag coefficient) for a set of design variables describing the wing geometry, while satisfying a number of specified constraints. This approach, though versatile, is still quite expensive, requiring several hours on a high-speed computer. The inverse design method of Shankar et al.[15] computes the wing geometry corresponding to a specified pressure distribution. The method is based on the small disturbance theory and, though computationally simple, requires a priori knowledge of what constitutes a desirable and achievable pressure distribution. Sobieczky et al.[16] propose a novel design procedure that modifies the wing geometry to make it shock-free for transonic flight conditions. This method is especially attractive because *any* reliable analysis code may be modified to be a design algorithm by incorporating the fictitious-gas concept. Results for simple wing designs based on a small disturbance analysis code are presented in Ref. 16. Yu[17] applied the same technique in conjunction with the Jameson-Caughey full-potential finite-volume code, further demonstrating the applicability of the fictitious-gas approach.

In this paper, the Jameson-Caughey full-potential finite-difference code,[18] FLO-22, is selected as the analysis code to be coupled with Sobieczky's fictitious-gas concept. The choice is dictated by a correlation of experimental data and theoretical results obtained at the Lockheed-California Company and the studies conducted by other investigators.[19,20] The FLO-22 code has been found to be one of the most *cost-effective* transonic-flow codes for analyzing wings. The full-potential finite-volume codes require considerably more computational time for a marginal improvement in accuracy.

The shock-free design method based on FLO-22 code requires four steps that are described below. A number of wing geometries have been successfully redesigned by applying this design procedure, and results for two cases are presented here. This paper also includes a discussion of the modifications made to the analysis code to improve the accuracy of computations, especially near the plane of symmetry for swept wings.

Description of Design Method

The basic idea of the present design procedure is to modify the wing surface geometry beneath the supersonic region to produce shock-free transonic flow at design conditions. The mathematical formulation of the problem assumes a steady, inviscid, isentropic flow which can be adequately described by the well-known quasilinear full-potential equation:

$$(a^2-u^2)\Phi_{xx}+(a^2-v^2)\Phi_{yy}+(a^2-w^2)\Phi_{zz}$$
$$-2uv\Phi_{xy}-2uw\Phi_{xz}-2vw\Phi_{yz}=0 \quad (1)$$

The local speed of sound is related to the flow speed as

$$a^2=a_0^2-(k-1)q^2/2 \quad (2)$$

where

$$q^2=u^2+v^2+w^2 \quad (3)$$

Of course, the boundary conditions are to be appropriately specified.

The FLO-22 code solves a finite-difference approximation to the full-potential equation in a sheared parabolic coordinate system which is nearly conformally mapped in planes parallel to the plane of symmetry of the wing. The choice of the coordinate system is especially suitable for finite-difference formulation because the wing surface reduces to a portion of one boundary of the computational domain. Consequently, the representation of the Neumann boundary conditions is considerably simplified. In the transformed coordinate system X, Y, Z, Eq. (1) is rewritten as

$$AG_{XX}+BG_{YY}+CG_{ZZ}+DG_{XY}+EG_{XZ}+FG_{YZ}+R=0 \quad (4)$$

where G is the reduced potential defined by $G=\Phi-x\cos\theta-y\sin\theta$. The coefficients A,B,C,D,E,F, and R are functions of the speed of sound, the reduced potential and its first derivatives, and various geometric mapping quantities. The details of the coordinate transformations and the relaxation method of solving Eq. (4) are documented in Ref. 18. The FLO-22 code is widely used in the aircraft industry for analyzing lifting, swept wings and it is the starting point of the present design method. A complete design of advanced shock-free supercritical wing requires the following four steps.

A. Fictitious-Gas Calculation

The first step in the design procedure is to modify the analysis code by incorporating the fictitious-gas concept. As detailed in Ref. 16, the basic equations are made to retain their elliptic behavior even when the flow has accelerated to supersonic speeds. For FLO-22 formulation, this is accomplished most conveniently by altering the local speed of sound according to a fictitious-gas sound speed law that renders the flow locally subsonic. Thus it is required that $a_f>q$ when $q>a_*$. The main consideration in choosing the sound speed law is that the fictitious mass flux matches the real mass flux at the sonic surface. Examples of the laws which satisfy these requirements[21] are

$$a_f^2=q^2/P \qquad P<1 \quad (5a)$$

$$=q^2(q/a_*)^L \qquad L>0 \quad (5b)$$

$$=q^2+\mu(q^2-a_*^2)^L \qquad \mu,L>0 \quad (5c)$$

Because the full-potential equation coupled with Eq. (5) is elliptic, the resulting solution is correct in all subsonic regions up to and including the sonic surface separating the real-gas subsonic flow from the fictitious-gas region. The shape and extent of the sonic surface depend upon the choice of the initial wing geometry, the sound speed law, and the values of the parameters in Eq. (5). The flow variables within the fictitious-gas region are discarded and the data on the sonic surface are saved for the next step.

B. Real-Gas Supersonic-Flow Calculation

The sonic surface data are used to calculate the correct real-gas flow inside the supersonic bubble bounded by the wing surface and the sonic surface. The method of characteristics is the most accurate and reliable technique, but it is not directly applicable to this ill-posed boundary value problem.[21] Therefore a suitable numerical algorithm that marches from the sonic surface toward the wing surface is desired.

The marching procedure for computing the real-gas supersonic flow may be formulated in either the physical or the transformed domain. However, in many cases, the sonic surface extends far enough around the leading edge that it becomes a double-valued function of the physical coordinates, which poses numerical difficulties in computations. In the present study, marching algorithm performs calculations in the transformed computational plane where the sonic surface is a single-valued function of the coordinates describing it. For the resulting hyperbolic marching problem, a system of first-order equations is formulated by rewriting Eq. (4) as

$$AU_X+BV_Y+CW_Z+DU_Y+EU_Z+FV_Z+R=0 \qquad (6)$$

and by utilizing two additional equations from the irrotationality condition, viz.,

$$U_Y-V_X=0 \qquad (7)$$

$$V_Z-W_Y=0 \qquad (8)$$

where

$$U\equiv G_X, \qquad V\equiv G_Y, \qquad W\equiv G_Z$$

To further facilitate the computational procedure, the curved sonic surface is mapped to a flat surface by setting $\bar{Y}=Y/Y_S(X,Z)$, as illustrated in Fig. 2. The marching can now be performed in $\bar{Y}$ direction only. In this new domain, the system of Eqs. (6-8) may be written as

$$\alpha\bar{U}_{\bar{X}}+\beta\bar{U}_{\bar{Y}}+\gamma\bar{U}_{\bar{Z}}=\delta \qquad (9)$$

where

$$\bar{U}=\begin{bmatrix} U \\ V \\ W \end{bmatrix} \qquad \alpha=\begin{bmatrix} A & 0 & 0 \\ 0 & -1 & 0 \\ 0 & 0 & 0 \end{bmatrix}$$

$$\beta=\begin{bmatrix} (D-\sigma_X A\bar{Y}-\sigma_Z E\bar{Y}) & (B-\sigma_Z F\bar{Y}) & -\sigma_Z C\bar{Y} \\ 1 & \sigma_X\bar{Y} & 0 \\ 0 & -\sigma_Z\bar{Y} & -1 \end{bmatrix}$$

$$\gamma=\begin{bmatrix} E & F & C \\ 0 & 0 & 0 \\ 0 & 1 & 0 \end{bmatrix} \qquad \delta=\begin{bmatrix} -R \\ 0 \\ 0 \end{bmatrix}$$

and

$$\sigma_X=\frac{\partial Y_S}{\partial X} \qquad \sigma_Z=\frac{\partial Y_S}{\partial Z}$$

Equation (9) is used to advance the solution from one $\bar{Y}$ level to the next one.

$$\bar{U}_j=\bar{U}_{j-1}+Y_s(\beta^{-1}\delta-\beta^{-1}\alpha\bar{U}_{\bar{X}}-\beta^{-1}\gamma\bar{U}_{\bar{Z}})_j\Delta\bar{Y} \qquad (10)$$

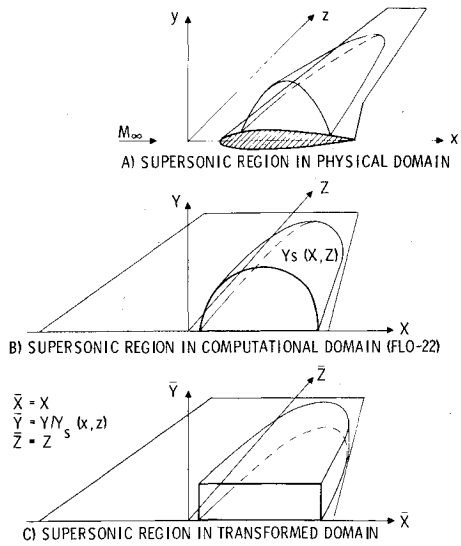

Fig. 2 Real-gas supersonic flow calculation.

The $\bar{X}$ and $\bar{Z}$ derivatives of $\bar{U}$ are calculated using central differences after smoothing the data at each level. The computation $\bar{U}$ proceeds until the original wing surface, $\bar{Y}=0$, is reached. The values of $\bar{U}$ on this surface will be used in the next step to modify the wing surface geometry.

Two difficulties may arise in the marching process just described. The first is that a limit surface may intervene between the sonic surface and the wing surface that renders the solution multivalued. In that case, no physically acceptable solution is possible with the initial data supplied. A change of sign of the determinant of matrix β indicates such an eventuality. A different fictitious-gas law or a different baseline wing may be required for the design procedure. The other difficulty is related to the ill-posed nature of the marching problem. The data given on the sonic surface are not in the usual domain of dependence for the hyperbolic problem. The marching procedure is, therefore, inherently unstable. However, meaningful solutions are obtained for moderate-to-high aspect-ratio wings, where the variations in spanwise direction are small compared to the chordwise variations.

C. Computation of the New Wing Shape

The supersonic-flow velocity distribution on the original wing surface calculated in the previous step does not satisfy the normal-flow boundary condition. Therefore a new wing geometry is determined such that it is a stream surface of the computed supersonic flow. The calculations are again performed in the computational plane where the original wing maps to a part of the $Y=0$ plane. Assuming that the new surface is given by $Y=Y_b(X,Z)$, the appropriate normal-flow boundary condition on the new surface is

$$q\cdot\nabla F=0 \qquad (11)$$

where

$$F=Y-Y_b(X,Z)=0 \qquad (12)$$

is the equation of the new surface. The velocity vector on this new surface may be written as

$$q=q_{Y=0}+(\partial q/\partial Y)_{Y=0}\cdot Y_b+\ldots \qquad (13)$$

The first term on the right-hand side of Eq. (13) is the supersonic-flow velocity vector on the surface of the original wing obtained from step B. The components of the derivative of the velocity vector used in the second term are numerically

evaluated using the results from step B. The higher-order terms in Eq. (13) are neglected. Substituting Eqs. (12) and (13) into Eq. (11) and ignoring the nonlinear terms and the terms of second order or higher in Y_b, a first-order, linear, partial-differential equation governing Y_b is obtained:

$$A_0 \frac{\partial Y_b}{\partial X} + B_0 \frac{\partial Y_b}{\partial Z} + C_0 Y_b = D_0 \tag{14}$$

The coefficients are functions of the velocity components on the original surface and the geometric transformation-related quantities. Equation (14) is integrated by the standard method of characteristics procedure, which gives

$$\frac{dX}{A_0} = \frac{dZ}{B_0} = \frac{dY_b}{D_0 - C_0 Y_b} \tag{15}$$

Equation (15) is numerically solved by marching in the X direction using

$$Z_{i+1} = Z_i + (B_{0_i}/A_{0_i})\Delta X \qquad \Delta X = X_{i+1} - X_i \tag{16}$$

and a predictor-corrector iteration for Y_b,

$$Y_{b_{\overline{i+1}}} = Y_{b_{i-1}} + 2\Delta X(D_{0_i} - C_{0_i} Y_{b_i})/A_{0_i}$$

$$Y_{b_{i+1}} = Y_{b_i} + \frac{\Delta X}{2}\left\{\frac{D_{0_i} - C_{0_i} Y_{b_i}}{A_{0_i}} + \frac{D_{0_{i+1}} - C_{0_{i+1}} Y_{b_{\overline{i+1}}}}{A_{0_{i+1}}}\right\} \tag{17}$$

The results are interpolated to compute the desired values at the grid points. The physical ordinates of the new wing geometry are obtained by transforming the Y_b values back to the physical domain.

D. Verification of the New-Wing Geometry

The final step of the design procedure is to analyze the new wing by the finite-difference FLO-22 code to ensure that the new geometry does indeed provide shock-free flow. Such verification is essential because the marching problem described in step B is ill-posed.

An improved version of FLO-22 code has been used in the applications of the design method detailed above. The improvements made to the original analysis code are, therefore, described below prior to discussing the results of the present study.

Improvements to the Analysis Code

In the course of the present investigation, an inaccuracy was uncovered in the FLO-22 code used at the Lockheed-California Company that causes significant flow across the plane of symmetry for swept wings. The computation of the velocity components using the final values of G has been modified to correct this problem. In addition, an attempt has been made to simulate the effect of a fuselage on the flow over the wing. These modifications have been incorporated in the analysis code as described below.

Flow Across the Plane of Symmetry

In the FLO-22 code, central differences are used to calculate all the first derivatives of the reduced potential G from which the velocity components can be readily computed. At the grid points where flow is subsonic, central differences are used to approximate the second derivatives also. A directional bias is appropriately added to Eq. (4) when the local flow is supersonic by using a rotated difference scheme. On the plane of symmetry (X-Y plane) and the wing surface (part of X-Z plane), the boundary-condition equations are approximated by central differences. However, the solution based on a relaxation scheme using central differences becomes unstable for moderately swept wings owing to the nonorthogonality of the coordinate system. To stabilize the solution, the G_X term in the plane of symmetry boundary condition is evaluated by

$$G_X = 0.5(G_X^U + G_X^D) \tag{18}$$

where the derivative in the upwind direction, G_X^U, is in the image plane and the derivative in the downwind direction, G_X^D, is in the flow plane adjacent to the plane of symmetry.[18]

It is found that the above formulation, while stabilizing the code, produces significant flow across the plane of symmetry for swept wings, as shown in Fig. 3, where the components of the velocity vector are computed by central differencing the potential G. The flow across the plane of symmetry is eliminated when Eq. (18) is used for the final computation of velocity component w. The values of the surface-pressure coefficient at the plane of symmetry are accordingly modified.

Wing-Fuselage Interference Effect

The original FLO-22 code is intended for an inviscid analysis of isolated wings only. There are full-potential transonic-flow codes that can analyze wing-body combinations, but they are very expensive to use. The authors, therefore, attempt to simulate the effect of fuselage on the wing while using the FLO-22 code for analysis. This is accomplished by changing the usual no-flow boundary condition, $w=0$, imposed on the plane of symmetry to an amended boundary condition, $w=w_F(x,y,z)$. The term w_F corresponds to the normal component of the perturbation velocity at the grid points on the plane of symmetry due to the fuselage. This perturbation flowfield is composed of two parts: 1) the flowfield due to a finite cylinder representing the fuselage with its axis parallel to the axial component of the freestream, and 2) an infinite cylinder of appropriate radius placed normal to the cross-flow component of the freestream. The former is simulated by distributing compressible sources and sinks along the axis of the finite cylinder; and the singularity strength is proportional to the axial rate of change of area of the fuselage. The latter is computed by the standard analytical formulation of an infinite cylinder in a uniform onset flow. The computed velocity component, w_F, at the grid points on the plane of symmetry is specified at the beginning of the relaxation solution and remains unchanged thereafter. The effect of including the fuselage induced flow is found to be more pronounced on the inboard stations, which is to be expected.

In addition to the two modifications described above, the improved version of FLO-22 code may be coupled with a boundary-layer calculation in an iterative manner. The computed displacement thickness for a specified potential flow pressure distribution is added to the wing surface. The

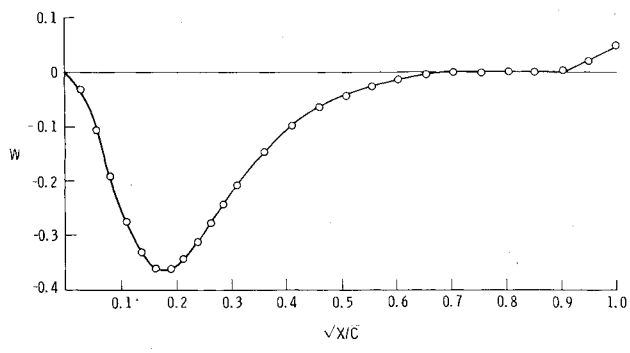

Fig. 3 Normal component of velocity at the plane of symmetry for a swept wing using the FLO-22 code.

FLO-22 code then analyzes the new wing geometry. This procedure of simulating the viscous effects has been found to be reasonably accurate for a variety of wings having attached flow. Of course, more accurate and efficient boundary-layer calculation methods than currently available are desirable.

The improved FLO-22 code, incorporating the viscous effect, the fuselage effect, and the modified computation of the velocity components at the plane of symmetry, gives pressure distributions that are in better agreement with the experimental data than the original FLO-22 results. This is

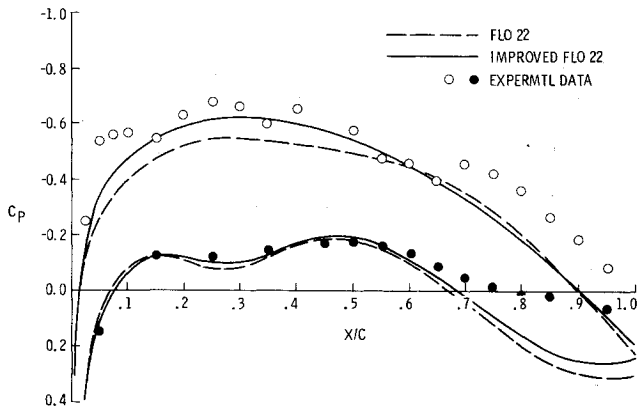

Fig. 4 Comparison of computed pressure coefficient variation for the FLO-22 code and its improved version with experimental data for a typical transport aircraft swept-back wing; $2z/b = 0.038$, $M_\infty = 0.84$, $C_L = 0.5$.

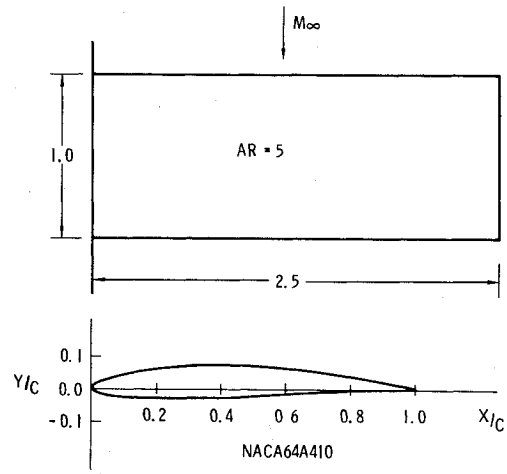

Fig. 5 Planform and the root section of an unswept, constant-chord wing of aspect ratio 5.

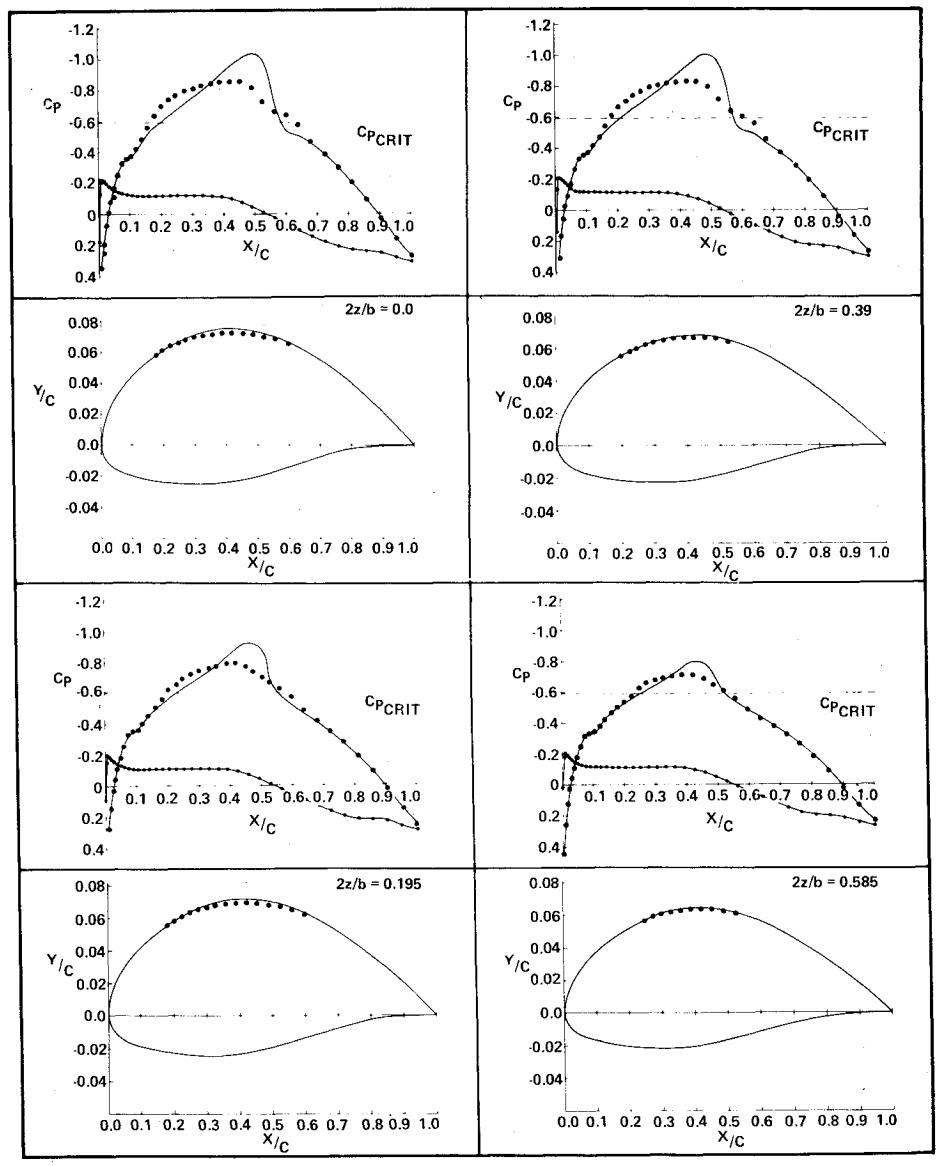

Fig. 6 Comparison of original (−) and shock-free (···) pressure distributions and wing cross-sections at four span stations for the wing shown in Fig. 5.

illustrated in Fig. 4 by the comparison of computational results for a typical transport wing section and the corresponding experimental results.

Computational Results

The present design technique was tested by applying it to an unswept, constant-chord wing of aspect-ratio 5 with an NACA 64A series airfoil section (see Fig. 5). The thickness ratio tapers linearly from 10% at the root to 7.5% at the tip. The design lift coefficient is 0.39 at the freestream Mach number of 0.75. The analysis code FLO-22 uses a moderate-sized fine grid having 129, 18, and 27 grid points in the X, Y, and Z directions, respectively. The code was modified to incorporate the sound speed law given by Eq. (5c), with $\mu = 1$ and $L = 5$. The sonic surface resulting from the fictitious-gas calculations extended outboard to approximately 70% of the wing half-span. The sonic surface data were used to modify the wing geometry beneath the supersonic region. The flow past the new wing was then analyzed by FLO-22. The computed pressure distributions on the original and modified wings, along with their section geometries, are shown in Fig. 6 at four span stations. It is clear from the comparison of these results that the modified wing is indeed shock-free. The computed inviscid drag of the modified wing is approximately 10% less than that of the original wing for the same total lift.

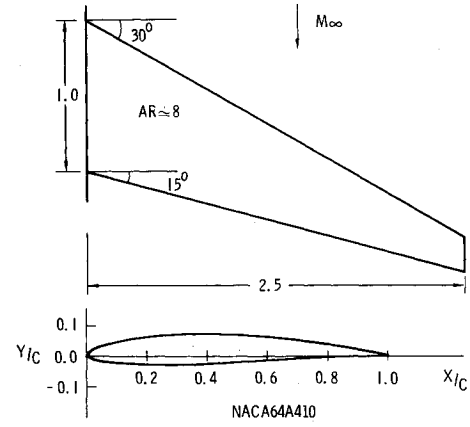

Fig. 7 Planform and the root section of a swept, tapered wing of aspect ratio 8.

A more practically meaningful wing geometry is considered for the next application of the design technique. As shown in Fig. 7, the wing section is NACA 64A410, the leading-edge sweep is 30 deg and the trailing-edge sweep is 15 deg. The wing has an aspect ratio of 8 with the twist varying from 3 deg at the root to zero outboard of the midspan. The design lift coefficient is 0.63 at 0.8 Mach number. For this case, the fictitious-gas model corresponds to Eq. (5b) with $L = 5$ and

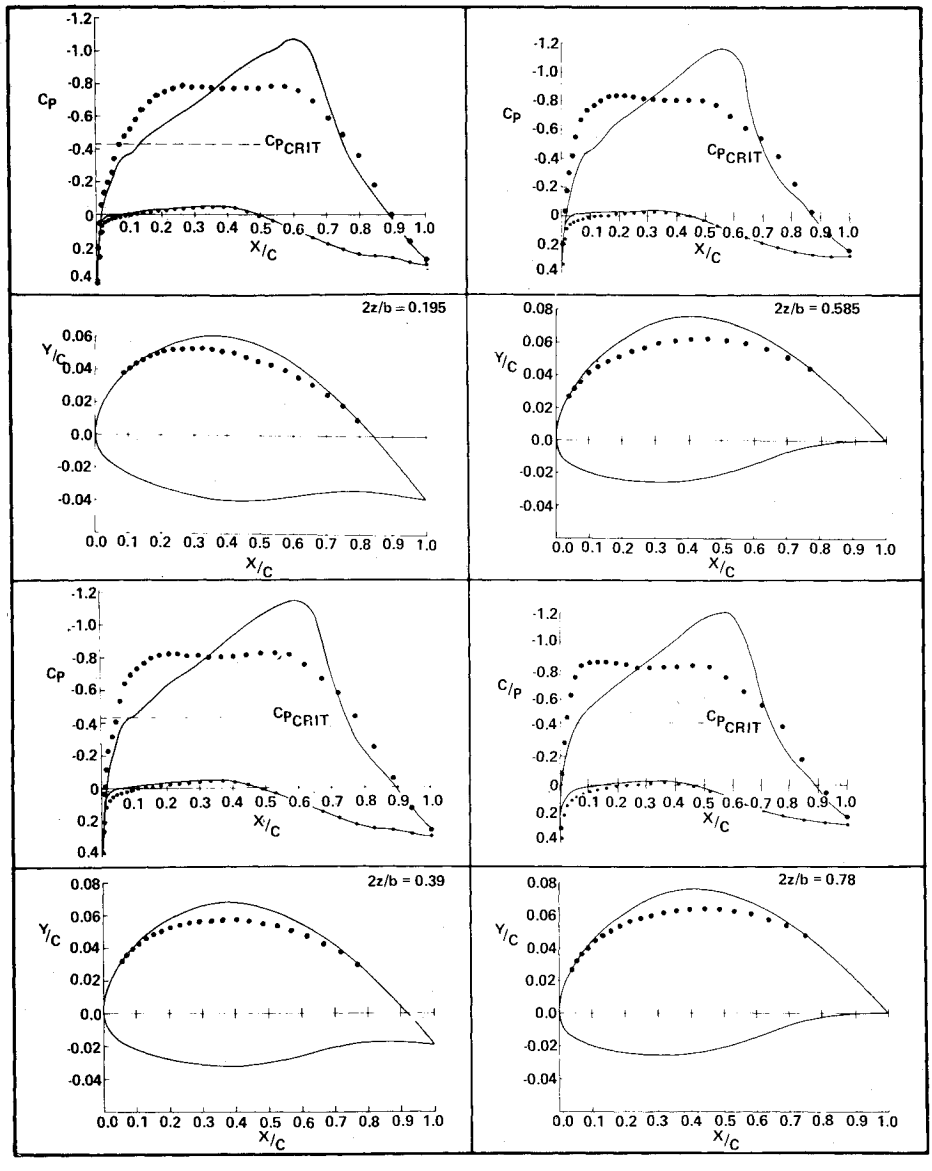

Fig. 8 Comparison of original (–) and shock-free (···) pressure distributions and wing cross-sections at four span stations for the wing shown in Fig. 7.

the resulting sonic surface extends all the way to the tip. Figure 8 compares the computed chordwise pressure distributions on the original and the modified wings, along with their section geometries, at four span stations. The shock waves on the upper surface of the original wing are eliminated by modifying the surface geometry. This results in a possible reduction of total inviscid drag by approximately 35%. It should be noted that the computationally predicted drag reduction may not be quantitatively realizable in practice. Nevertheless, the pressure distributions on the modified wing sections indicate that the wave drag would be substantially less owing to the elimination of shock wave. In addition, the shock-wave-induced boundary-layer separation losses will be avoided.

The selection of the two wings designed in this study is based on the following considerations. The most important one is that similar wing geometries have been used in other investigations[16,17,21] for successful development of shock-free design procedures. The results of the present technique may, therefore, be qualitatively compared with those of the other computational methods. Moreover, it is suggested by Fung et al.[21] that the original wing should preferably have reasonable upper surface curvature. Then, the intersection of the sonic surface with the wing surface is acute, which reduces the likelihood of a limit surface intervening between the sonic surface and the wing surface. The NACA64A4 series airfoils meet these requirements satisfactorily.

During this investigation, it was observed that the new wing shape resulting from a streamwise integration of Eqs. (16) and (17) over the supersonic part does not close at the aft end. This is not completely surprising. Unlike the two-dimensional case where the new shape has the same slope and, at least theoretically, the same curvature as the original shape at the sonic points,[16] an exact closure may not be guaranteed in three dimensions.[17] In the results given here, the computed new wing geometry is rotated about an appropriate pivot point to define a closed shape. At the present time, the forward point of intersection of the sonic surface with the wing surface is chosen as the pivot point. The authors are further studying this problem to arrive at the best solution.

Both of the cases discussed here correspond to inviscid transonic flow. The effect of boundary layer can be included relatively easily because the surface pressures for fictitious-gas calculations are usually close enough to those of the final design that the boundary-layer displacement thickness may be computed using the fictitious-gas pressures. As mentioned earlier, the analysis code is capable of handling such an inviscid-flow/boundary-layer interaction.

Concluding Remarks

A cost-effective computational procedure for the design of shock-free three-dimensional wings having desirable transonic-flow aerodynamic characteristics has been described. The method uses the FLO-22 code as the basic analysis tool, which has been improved by modifying the computation of the velocity components at the plane of symmetry. The code used here is also capable of simulating wing-fuselage interference effects. The design procedure couples this analysis code with the fictitious-gas concept. Results for shock-free design of two wings, one rectangular and the other swept, are presented. In both cases, the shock waves associated with original geometries and flows have been eliminated. The resulting improvement in the value of the range factor is an important consideration in improving the cruise efficiency of the transport aircraft.

Acknowledgments

This work is supported by the Lockheed-California Company Independent Research and Development Program. The authors wish to thank Barnaby Wainfan and J. Scott Reaser of the Lockheed-California Company for their assistance in modifying the transonic-flow analysis code.

References

[1] Whitcomb, R.T., "Review of NASA Supercritical Airfoils," Ninth International Congress on Aeronautical Sciences, Haifa, Israel, 1974.

[2] Pearcy, H.H., *Advances in Aeronautical Sciences,* Vol. 3, 1962, pp. 277-322.

[3] Nieuwland, G.Y., "Transonic Potential Flow Around a Family of Quasi-Elliptical Aerofoil Sections," NLR-TR-T-172, 1967.

[4] Bauer, F., Garabedian, P.R., and Korn, D.G., *Supercritical Wing Sections III,* Springer-Verlag, New York, 1977.

[5] Sobieczky, H., *Symposium Transsonicum II,* Springer-Verlag, Gottingen, 1975.

[6] Boerstoel, J.W., "Design and Analysis of a Hodograph Method for the Calculation of Supercritical Shock-Free Airfoils," NLR-TR-77046U, 1977.

[7] Hicks, R.M., Murman, E.M., and Vanderplaats, G.N., "An Assessment of Airfoil Design by Numerical Optimization," NASA TMX-3092, 1974.

[8] Steger, J.L. and Klineberg, J.M., "A Finite-Difference Method for Transonic Airfoil Design," *AIAA Journal,* Vol. 11, May 1973, pp. 628-635.

[9] Tranen, T.L., "A Rapid Computer Aided Transonic Airfoil Design Method," AIAA Paper 74-501, 1974.

[10] Carlson, L.A., "Transonic Airfoil Design Using Cartesian Coordinates," NASA CR-2578, 1976.

[11] Shankar, V., Malmuth, N.D., and Cole, J.D., "Computational Transonic Airfoil Design in Free Air and a Wind Tunnel," AIAA Paper 78-103, 1978.

[12] Volpe, G., "Two-Element Airfoil System Designs: An Inverse Method," AIAA Paper 78-1226, 1978.

[13] Hicks, R.M. and Henne, P.A., "Wing Design by Numerical Optimization," AIAA Paper 77-1247, 1977.

[14] Lores, M.E., Smith, P.R., and Hicks, R.M., "Supercritical Wing Design Using Numerical Optimization and Comparison with Experiment," AIAA Paper 79-0065, 1979.

[15] Shankar, V., Malmuth, N.D., and Cole, J.D., "Computational Transonic Design Procedure for Three-Dimensional Wings and Wing-Body Combinations," AIAA Paper 79-0344, 1979.

[16] Sobieczky, H., Yu, N.J., Fung, K.-Y., and Seebass, A.R., "New Method for Designing Shock-Free Transonic Configurations," *AIAA Journal,* Vol. 17, July 1979, pp. 722-729.

[17] Yu, N.J., "Efficient Transonic Shock-Free Wing Redesign Procedure Using a Fictitious Gas Method," *AIAA Journal,* Vol. 18, Feb. 1980, pp. 143-148.

[18] Jameson, A. and Caughey, D.A., "Numerical Calculation of the Transonic Flow Past a Swept Wing," New York University ERDA Report COO-3077-140, June 1977.

[19] Bhately, I.C., Mann, M.J., and Ballhaus, W.F., "Evaluation of Three-Dimensional Transonic Methods for the Analysis of Fighter Configurations," AIAA Paper 79-1528, 1979.

[20] Hinson, B.L. and Burdges, K.P., "Evaluation of Three-Dimensional Transonic Codes Using New Correlation-Tailored Test Data," *Journal of Aircraft,* Vol. 18, Oct. 1981, pp. 855-861.

[21] Fung, K.-Y., Sobieczky, H., and Seebass, A.R., "Shock-Free Wing Design," *AIAA Journal,* Vol. 18, Oct. 1980, pp. 1153-1158.